Structural Stability of Polypeptide Nanofilms under Extreme Conditions

Bingyun Li, Joshua Rozas,[†] and Donald T. Haynie*

Bionanosystems Engineering Laboratory, Center for Applied Physics Studies, Biomedical Engineering and Physics, P.O. Box 10348, Louisiana Tech University, Ruston, Louisiana 71272, and Department of Chemical Engineering, Box 44130, University of Louisiana, Lafayette, Louisiana 70504-4130

Self-assembly of designed peptides is a promising area of biomaterials research and development. Here, polypeptide nanofilms have been prepared by electrostatic layer-by-layer self-assembly (LBL) of cysteine (Cys)-containing 32mers designed to be oppositely charged at neutral pH, and structural stability of the films has been probed by subjecting them to various extreme physical and chemical conditions. The results suggest that although electrostatic attraction plays a key role in strengthening polypeptide films, stability is inversely related to absolute net charge of the supramolecular complex. This behavior is similar to the typical behavior of small globular proteins. Film structure is very stable in organic solvent and, when dehydrated, at extreme temperatures. Such stability is in marked contrast to the behavior of proteins, which tend to denature under comparable conditions. Similar to proteins, peptide nanofilms cross-linked by disulfide (S−S) bonds are considerably stronger than films stabilized by electrostatic, van der Waals, or hydrophobic interactions alone. This effect is particularly evident at extremes of pH and at elevated temperature when the film is hydrated. These results, the great variety of possible peptide structures, the inherent biocompatibility of L-amino acids, and current applications of thin films in commercial products together suggest that polypeptide films are promising for the development of new or enhanced products in food technology, drug delivery and medical device coatings, and biomaterials.

Introduction

Polyelectrolyte multilayer film formation and structure have been studied in considerable depth from the standpoints of polyacid−polybase interaction and electrostatic attraction (*1−3*). The apparent simplicity and inherent complexity of the method and its demonstrated suitability for programmatic formation of thin organized coatings have attracted attention since the early 1990s (*4−7*). Numerous applications are being developed in a range of areas, including some of interest to medicine, e.g., artificial membranes, antimicrobial coatings, and microcapsules (*8−10*).

A variety of biocompatible polyelectrolytes, including synthetic polyions, biomacromolecules such as DNA and polypeptides, enzymes, and viruses, dendrimers, and colloids, have been incorporated into multilayer systems (*1, 11, 12*). Examples are poly(L-lysine)/alginate films for use as nonadhesive barriers (*13*) and dextran/chitosan films for anticoagulation or procoagulation (*14*). Little research, however, has been done with designed polypeptide chains. This is surprising, as well-known natural materials such as spider silk, silkmoth eggshells, hair, and tendons are made largely of protein.

A major concern in developing polyelectrolyte multilayers for practical use is stability of film structure in different environments. A film could show an undesirable tendency to disintegrate under certain physical or chemical conditions (*15, 16*). Film stability could depend on solvent, pH, or temperature. Obvious advantages for technology commercialization will include being able to tailor film stability to a specific application.

Usually, polyelectrolyte multilayer formation is based mainly on electrostatic attraction. Hydrogen bonds and hydrophobic interactions also can be involved, the extent depending on the polymers involved. Electrostatic interactions are noncovalent in nature, but the contribution of an ion pair to free energy can be as high as 60 kJ/mol, perhaps higher in some cases. Covalent bonds are even stronger, up to ca. 400 kJ/mol for σ bonds. Chemical cross-linking therefore should further stabilize a polyelectrolyte multilayer film and could influence the adhesive properties of biological cells by changing the bulk modulus of the film and its stiffness (*17*). Exploiting the full potential of polypeptide films will require understanding the relationship between peptide design, film architecture, microscopic peptide structure, and assembly conditions on one hand and macroscopic physical, chemical, and biological film properties on the other hand.

Here, we have investigated the stability of S−S cross-linked and non-cross-linked polypeptide multilayer films in various kinds of harsh environment: dehydrated, strong base, strong acid, dimethylformamide (DMF), high temperature, and low temperature. Film structure and stability were analyzed by circular dichroism spectroscopy (CD) and UV spectroscopy (UVS). Results indicate that the secondary structure of multilayer films self-assembled from Cys-containing 32mer peptides can be stable under a broad range of physical and chemical environments. Film behavior is compared to that of small globular proteins under comparable conditions. The expectation that S−S cross-linked films are more stable than non-cross-linked ones has been confirmed throughout the pH range.

Experimental Section

Film Materials. Peptide 1 [(KVKGKCKV)₃KVKGKCKY] and Peptide 2 [(EVEGECEV)₃EVEGECEY] were prepared by solid-phase F-moc chemistry using the Advanced ChemTech

* To whom correspondence should be addressed. Tel: +1-318-257-3790. Fax: +1-318-257-2562. Email: haynie@latech.edu.

† University of Louisiana.

Table 1. Buffers for Assessing Film Stability

buffer[a]	pH
KCl−HCl	1.0, 1.5, 2.0
glycine	3.0
acetate	5.0
tris	7.4
glycine	9.0
phosphate	11.0
KCl−NaOH	12.0, 12.5, 13.0

[a] All buffers were 10 mM with 20 mM NaCl and 0.1% NaN_3.

Apex 390 peptide synthesizer (USA) at Louisiana Tech. Synthesis products were lyophilized, analyzed by mass spectrometry (Louisiana State University, Baton Rouge) and HPLC, and stored at −20 °C. All other chemicals were from Sigma (USA). Stock aqueous solutions of peptides were prepared at concentrations of 2 mg/mL and stored at 4 °C. The buffer for all assembly experiments was 10 mM Tris-HCl, 20 mM NaCl, 0.1% NaN_3, pH 7.4.

Film Assembly. Ten-bilayer films were prepared by sequential immersion of a quartz slide or SiO_2 wafer in solutions of Peptide 1 and of Peptide 2 (*16, 18*). After deposition of polymers for 20 min, substrates were rinsed with buffer and dried with a gentle stream of N_2 gas. Quartz crystal microbalance (QCM) (Agilent 53131A 225 MHz universal counter, USA) and UVS (Shimadzu UV-1650 PC spectrophotometer, Japan) were used to monitor stepwise deposition of polypeptides on silver-coated resonators (Sanwa Tsusho Co. Ltd, Japan) and quartz slides, respectively. Films were oxidized for S−S cross-linking by immersion in 20% dimethyl sulfoxide, 1 μM $MnCl_2$, 10 mM Tris, 20 mM NaCl, 0.1% NaN_3, pH 7.5, overnight at ambient temperature. A series of 10 mM buffer solutions containing 20 mM NaCl and 0.1% NaN_3 were prepared to study the stability of peptide films as a function of pH (Table 1). Different buffers were used because none provides sufficient buffering capacity throughout the entire pH range studied in this work.

Film Disassembly. The stability of polypeptide multilayer films was monitored by UVS and CD. Each UVS experiment involved four samples, two with cross-links and two without. A cross-linked sample and a non-cross-linked sample were immersed sequentially in aqueous solutions at pH 7.4, 5.0, 3.0, 2.0, 1.5, or 1.0 for 30 min per solution. The other two samples were immersed in solutions at pH 7.4, 9.0, 11.0, 12.0, 12.5, or 13.0. The amount of peptide retained on the substrate following pH shift was determined by absorbance at 221 nm, where the peptide bond absorbance is approximately independent of backbone conformation (*19*). Cross-linked and non-cross-linked film stability was also monitored by far-UV CD (Jasco J-810 spectropolarimeter, Japan). The far-UV signal is sensitive to peptide backbone conformation. Samples were cooled for 10 min at −196 °C in liquid nitrogen; dehydrated and heated for 1 h at 100 °C; dehydrated and hydrated by immersion in buffer at pH 1.5, 7.4, or 12.0 for various lengths of time at about 25 °C; or dehydrated and hydrated by immersion in buffer at pH 5.5 for up to 5 h at 95 °C. In each CD experiment, 50−100 scans were collected and averaged. Deconvolution of the far-UV CD spectra into contributions from α helix, β sheet, β turn, and random coil was done using the CD Pro software suite (program CONTINLL) (*20*).

Film Surface Characterization. Ten-bilayer peptide films on SiO_2 were characterized by atomic force microscopy (AFM) (Quesant Instrument Corp., USA) in tapping mode at ambient temperature, before and after immersion of the film in acidic solution at pH 1.5. Data were collected at given time points for up to 3 h. Each measurement required removal of the plates from solution and drying with N_2 gas.

Results and Discussion

Modeling: Visualizing the Interacting Polypeptides. Molecular models of Peptide 1 and Peptide 2 in extended conformation are shown in Figure 1. All charged side chains point in the same direction, all aliphatic ones in the opposite direction. Side chain orientation is the same in classical β pleated sheet conformation. Both peptides have a contour length of ca. 9.4 nm and a "thickness" of ca. 1.0 nm. The structures differ in net charge: Peptide 1 is positive at neutral pH whereas Peptide 2 is negative. The absolute charge density is about 0.5 electronic charges per residue at pH 7.4. The peptides bind to each other in a multilayer film by electrostatic attraction, the mechanism of electrostatic LBL. Other types of interaction, however, will contribute to film assembly and stability.

QCM and UVS: Monitoring Film Assembly and Dissociation. Sequential deposition of Peptide 1 and Peptide 2 was monitored by QCM and UVS. Figure 2a shows that the resonant frequency of the dried film on a resonator decreased with number of adsorption steps. This observation implies that peptide was deposited during each step of the film assembly process (*21*). The frequency change was approximately linear and proportional to the number of bilayers, though more Peptide 1 than Peptide 2 adsorbed per deposition step. The plateau formed in each assembly step reflects the self-limiting nature of polyelectrolyte adsorption: charge enables deposition by electrostatic attraction between but limits it by repulsion within a layer. The deposition process approaches quasi-equilibrium in a local Gibbs free energy minimum, but the process is best
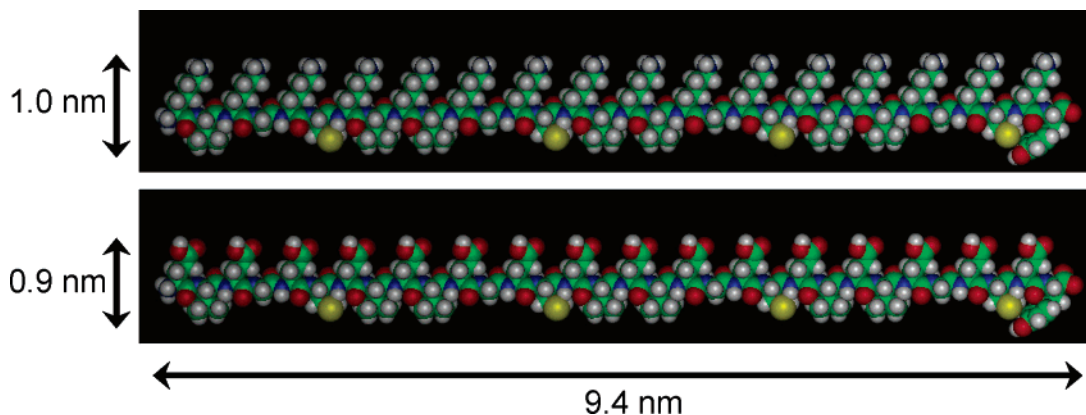

Figure 1. Molecular models of Peptide 1 and Peptide 2. The hydrophilic side chains (lysine, Peptide 1; glutamic acid, Peptide 2) point upward, the hydrophobic side chains downward. The sulfur atoms of the cysteine side chains are shown in yellow. The models were built using Biopolymer and displayed with InsightII (Accelrys, USA).
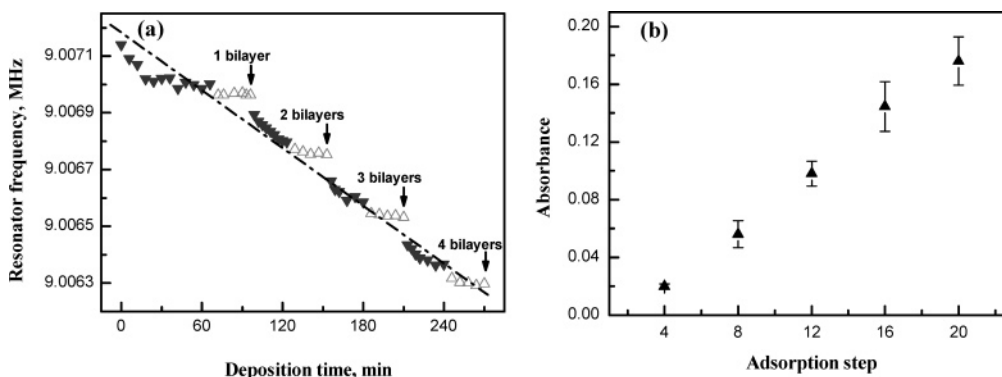
Figure 2. Kinetics of polypeptide film assembly. (a) QCM. Filled symbols represent deposition of Peptide 1, open symbols Peptide 2. Each deposition cycle tends toward a plateau in resonant frequency, reflecting the self-limiting nature of polyelectrolyte adsorption. The process, however, involves the kinetic trapping of molecules; adsorption is essentially irreversible under usual conditions. That assembly occurs at all reflects the role of electrostatic attraction in assembly. The mass sensitivity constant for conversion of frequency shift into mass deposited is 1.83×10^8 Hz cm^2 g^{-1}. The dashed line is included as a visual aid. (b) UVS. This method indicates the "optical mass" of adsorbed material. Mass deposition is an approximately linear function of adsorption step. Data were collected at 221 nm.
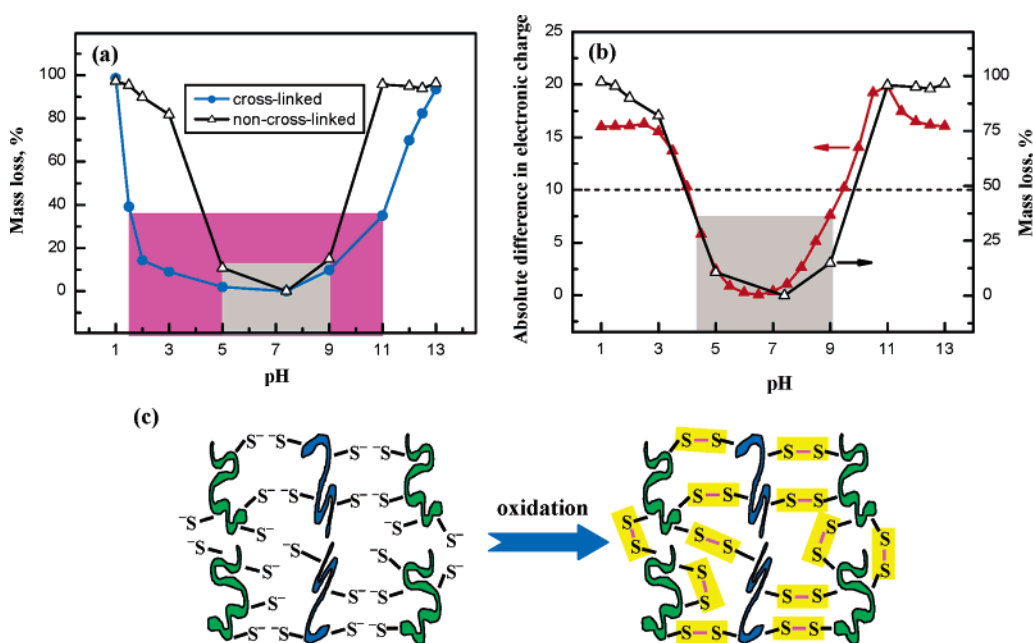

Figure 3. Multilayer film stability monitored by UVS. (a) Percentage of peptide loss from substrates after pH shift. Absorbance was measured at 221 nm. The highlighted areas represent the pH ranges over which the films were stable. Grey: cross-linked. Magenta: non-cross-linked. (b) Calculated absolute net charge between one molecule of Peptide 1 and one molecule of Peptide 2 versus pH. No correction of pK_a was made for environmental effects. The stability of the non-cross-linked sample is shown for comparison. The corresponding spectra are displayed in Figure 5S in Supporting Information. (c) Schematic illustration of the stabilizing mechanism of S−S cross-linking. A polypeptide multilayer film can be made "competent" for "natural" covalent cross-linking by inclusion of the amino acid cysteine. Interlayer and intralayer S−S bonds form upon film oxidation, "locking" the polypeptide supramolecular structure into place and increasing film stability. Disulfide bond formation is reversible.

described as being under kinetic control. The length of an adsorption step is a process control variable. The assembly of Peptide 1 and Peptide 2 on quartz slides was also monitored by UVS at 221 nm. Figure 2b shows that the amount of material deposited on the substrate increased approximately linearly with number of bilayers, consistent with QCM analysis.

S−S cross-linking has been adapted as a biomimetic approach to strengthening the structure of materials. It is used, for example, to enhance the structural integrity of peptide-amphiphile nanofibers (*22*). It is also involved in the vulcanization of rubber, important for the reliability and longevity of tires. In earlier work we showed that S−S bonds stabilize multilayer polypeptide films (*23*). Here, the influence of S−S bonds on film stability has been tested over a wide range of physical and chemical conditions.

Two polypeptide film samples, one cross-linked and the other not, were immersed for 30 min in aqueous solution buffered at

a pH between 1.5 and 13. Absorbance of the films at 221 nm was measured to detect and quantify loss of material. Baselines were subtracted from respective spectrophotometer readings and converted to percentage material lost. Figure 3a shows that film disintegration was large for non-cross-linked samples below pH 5 or above 9: films were unstable when the pH differed by more than 2 units from neutral. By contrast, cross-linked samples lost less than 40% of their material in the range pH 1.5−11 and less than 20% in the range pH 2−9.

Deprotonation of NH$_3^+$ groups in Peptide 1 and protonation of COO$^-$ groups in Peptide 2 in a highly basic or highly acidic environment, respectively, will change the charge density of the polypeptides and the film. The results presented here imply that electrostatic interactions which stabilize the films thus are weakened at low or high pH, and film disintegration results. Figure 3b shows the calculated absolute charge on the Peptide 1/Peptide 2 system in a 1:1 molar ratio. The calculation was
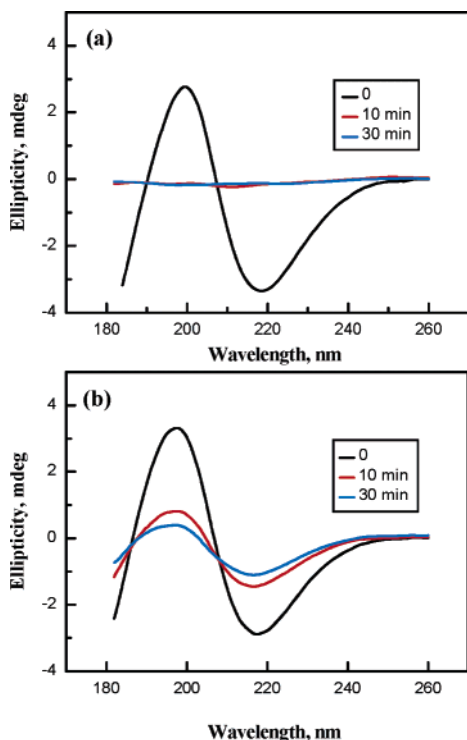
Figure 4. Peptide film stability at pH 12 as monitored by CD. Decrease in amplitude is indicative of destruction of secondary structure and loss of material. The non-cross-linked sample (a) was less stable than the cross-linked one (b).
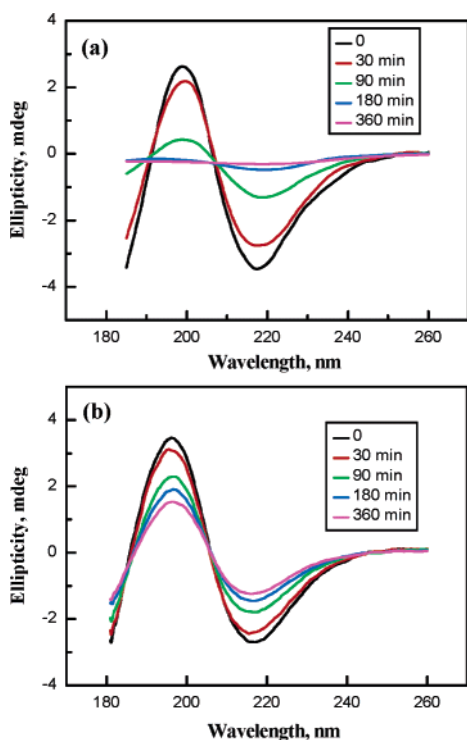

Figure 5. Peptide film stability at pH 1.5 as monitored by CD. The non-cross-linked sample (a) was less stable than the cross-linked one (b).

Figure 6. Peptide film stability in an aqueous medium (pH 5.5) at high temperature (95 °C) as monitored by CD. The non-cross-linked sample (a) was less stable than the cross-linked one (b).

Table 2. Comparison of Physical Properties of Peptide 1, Peptide 2, PLL, and PLGA

| | physical properties per residue | | | |
| | | secondary structure (average) | | |
polypeptide	approx charge at neutral pH	α helix propensity	β sheet propensity	% difference[a]
Peptide 1	+0.5	0.96	1.06	9 $\alpha < \beta$
Peptide 2	−0.5	1.05	1.03	2 $\alpha > \beta$
PLL	+1.0	1.13	0.80	29 $\alpha > \beta$
PLGA	−1.0	1.27	0.74	42 $\alpha > \beta$

[a] Calculated as (larger − smaller)/larger × 100.

the side chains titrate. The electrical potential energy of the two peptide system will have essentially the same profile for a fixed conformation. The comparison therefore suggests that the main source of stability of the multilayer films studied here is the electric force, consistent with interpretations of many previous polyelectrolyte LBL studies. At "low" absolute charge difference between molecules, the film is stable: mass loss was less than 50%. Stability was maximal near pH 7, where both peptides are charged but the absolute film charge is a minimum. At "high" absolute charge difference, repulsion between charged molecules in a layer becomes significant.

Figure 3a also implies that S−S cross-linking enhances polypeptide film stability at extreme pH, consistent with earlier work (23). The formation of S−S bonds in thin films is illustrated in Figure 3c. S−S bonds, being covalent, are less susceptible to environmental stress than noncovalent ionic interactions. Cross-linking prevents or retards film disintegration over a wide range of pH and requires large aggregates of polymer to act in concert when separating from the remainder of the film or the substrate. The collective effect of a large number of weak interactions can be quite strong, as for example with hydrogen bonds in globular protein stability.

Physical properties of polypeptide multilayer films can be compared with the well-known behavior of globular proteins.

based on microscopic dissociation constants for the purpose of qualitative comparison: no effect of environment on ionization was taken into account (e.g., 24). Obviously the actual situation is more complex, but the approach is a reasonable first approximation. As seen in the figure, the difference in net charge is small and minimal near neutral pH but large in regions where
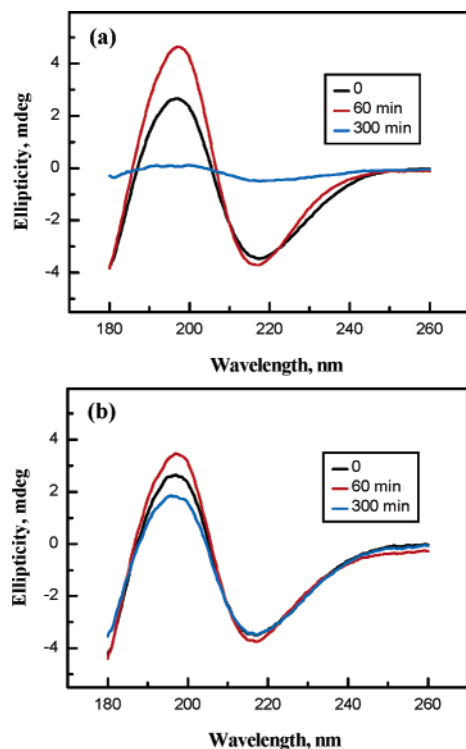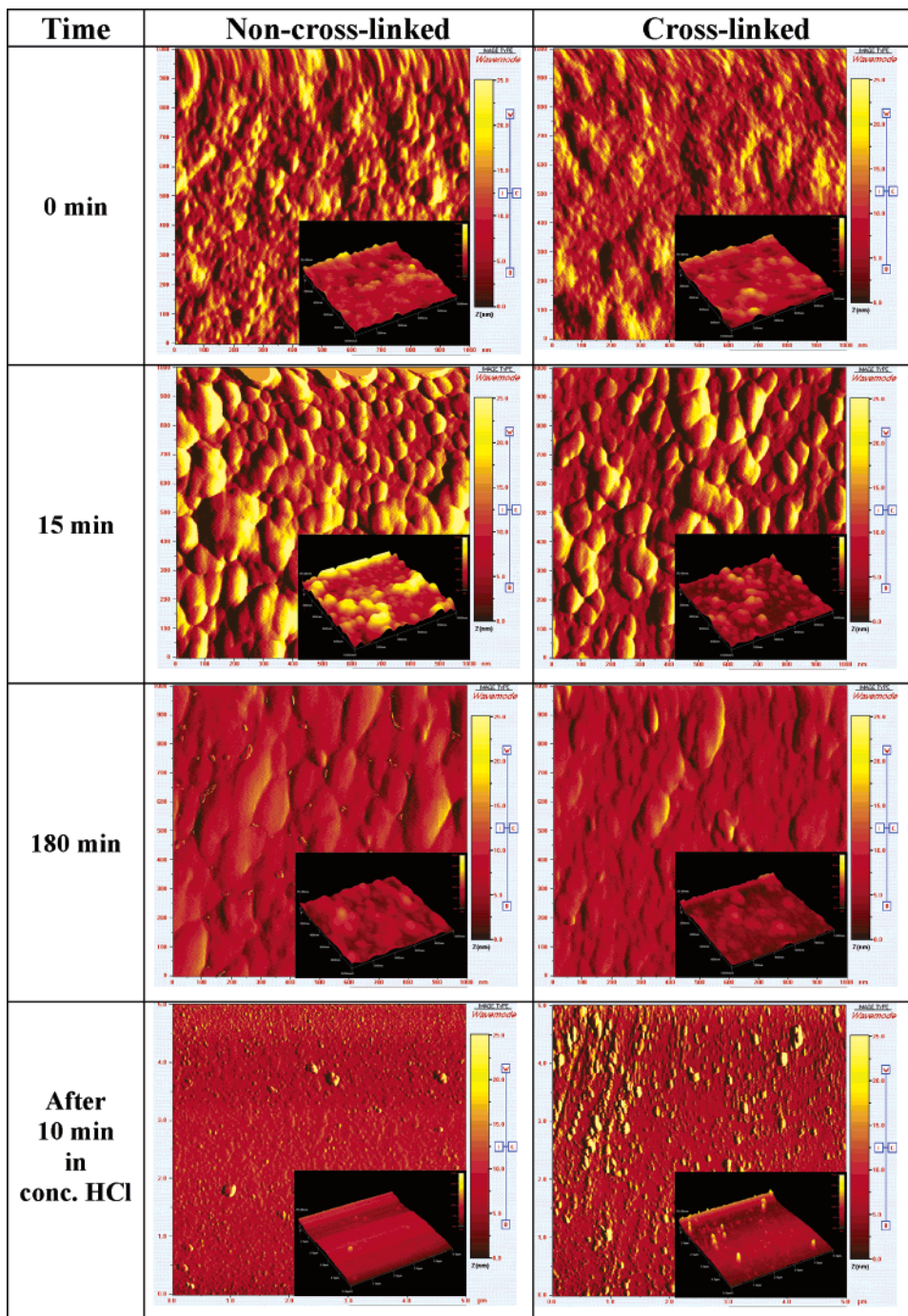
Figure 7. AFM micrographs of non-cross-linked (left) and cross-linked (right) peptide films. Immersion time in aqueous solution at pH 1.5 was 0, 15, or 180 min, followed by 10 min in concentrated HCl. The height scale is 25 nm throughout.

The native structure of a typical small globular protein will have a thermostability of 80 kJ/mol or less and therefore can be denatured by a change of environment, e.g., a rise in temperature or decrease of pH. A salt bridge can contribute to native state stability, but it will be disrupted at an extreme of pH as a result of side chain ionization. Maximal thermostability will likely be near the isoelectric point, in most cases near neutral pH, where the net charge and therefore electrical potential energy are zero; many proteins tend to denature below pH 5 or above 10 (*25*). This aspect of protein stability resembles the behavior of non-cross-linked multilayer peptide films studied here. The films are stable in the range pH 5−9, relatively far from the intrinsic pK_a of the glutamic acid or lysine side chain. S−S cross-linking resembles the behavior of proteins, too. An example is given by hen egg white lysozyme, the thermostability

of which at acidic pH depends substantially on the presence of native disulfide bonds (e.g., *26*).

CD: Determining Film Secondary Structure Content. Percentage change in signal amplitude during film disassembly followed closely that obtained by UVS (not shown). Figures 4 and 5 present far-UV spectra of (a) non-cross-linked and (b) cross-linked samples after exposure to extreme pH for a given time interval. Evidently, most of the material and structure was lost from the non-cross-linked sample lost within 10 min at pH 12 (Figure 4), and within 180 min at pH 1.5 (Figure 5). The change was substantially less extreme for the cross-linked sample under the same conditions.

Deconvolution of the CD spectra revealed that the most prevalent secondary structures in the peptide films studied here were β strands, even at extremes of pH (see table in Supporting

Information). The percentage of α helix present was small in all cases. There was no obvious change in film secondary structure content on change of conditions. This result differs from earlier work with poly(L-lysine) (PLL) and poly(L-glutamic acid) (PLGA) (*16*). PLL/PLGA films disintegrate at extremes of pH, though more readily at pH 12.0 than pH 1.5. These films also exhibit a significant reorganization of structure, on a time scale of minutes, on exposure to aqueous solution at pH ≤ 2.5 or pH ≥ 12.0, from β sheet to α helix. The difference in observed behavior between PLL/PLGA films and those studied here may reflect the probability of the different peptides involved to form a type of secondary structure. Calculated propensity per residue and other physical properties are given in Table 2. The PLL/PLGA system has much higher charge per residue at neutral pH and propensity to form an α helix than the Peptide 1/Peptide 2 system. Microscopic changes in film structure, due to changes in peptide primary structure, will give rise to differences in bulk film properties. The high propensity to form α helix in the PLL/PLGA system may explain the reorganization of the corresponding film secondary structure upon exposure to pH ≤ 2.5 or pH ≥ 12.0. As with PLL and PLGA, more rapid disintegration of Peptide1/Peptide 2 films occurred at pH 12.0 than pH 1.5, but there was no apparent change in the secondary structure content at extreme pH. In other words, the integrity of film structure was preserved under extreme conditions in the Peptide 1/Peptide 2 system. In this regard, the Peptide 1/Peptide 2 films differ from PLL/PLGA films and typical small globular proteins.

Figure 6a and b show the far-UV spectra of non-cross-linked and cross-linked samples, respectively, on exposure to aqueous solution (pH 5.5) at 95 °C for a given time period. Most globular proteins denature below this temperature for any choice of solvent. The non-cross-linked film at 95 °C lost its structural integrity after 300 min; the cross-linked sample was more stable. Immersion of the peptide films in neutral buffer at ambient temperature for 4 weeks resulted in no detectable loss of material, regardless of cross-linking (see Supporting Information, Figure S1).

Aliphatic side chains of proteins are more soluble in a nonpolar organic solvent than in water, so hydrophobic interactions between residues are weakened on a corresponding change of medium. Acetone, DMF, and methanol, for example, can denature proteins. Salt bridges and hydrogen bonds will contribute to the thermostability of an ordered conformation. The mechanism of denaturation under any conditions will involve disruption of noncovalent interactions. Formation of electrostatic interactions, hydrogen bonds, and van der Waals interactions is exothermic, and therefore such "bonds" are destabilized on heating. As a result, most proteins denature in the range 50−100 °C in an aqueous medium and at a lower temperature in a nonaqueous medium. Here, the stability of dehydrated peptide films was studied in organic solvent (DMF) and at temperatures ranging from −196 to 100 °C (see Supporting Information, Figures S2−S4). The results show that both cross-linked and non-cross-linked films are very stable under these conditions or that any changes in structure are highly reversible: dehydrated Peptide 1/Peptide 2 complexes preserve structural integrity under these conditions.

AFM: Assessing Film Surface Morphology. Surface morphology of the peptide films was characterized by AFM. Figure 7 shows micrographs of samples treated at pH 1.5 for a given length of time. All height scales are the same. Evidently, low pH treatment had a marked effect on surface morphology of the cross-linked film and the non-cross-linked film, increasing

roughness. After treatment at pH 1.5 for 180 min, less material was present in non-cross-linked samples than the cross-linked ones. Some non-cross-linked material remained, however, even after extensive treatment at acidic pH. It might be difficult to remove all peptide from the substrate once adsorbed, regardless of cross-linking. This resembles the stickiness of proteins. Substantially more material remained on the cross-linked sample than the non-cross-linked one after a defined period of time.

Conclusions

The structural stability of nanofilms made of custom-designed 32mer Cys-containing peptides has been tested under a broad range of physical and chemical conditions: neutral pH buffer, strong acid, strong base; organic solvent; hydrated, dehydrated; ambient temperature, low temperature, and high temperature. The stability and surface morphology of S−S cross-linked films and non-cross-linked films have been assessed using a combination of physical techniques (CD, UVS, and AFM). The results suggest that the electric force is the main one that stabilizes multilayer peptide films at ambient temperature in aqueous solution, despite the presence of a substantial amount of hydrophobic surface area on the peptides and apparently contrary to the view that globular proteins are stabilized largely by hydrophobic interactions. S−S bonding results in the formation of a three-dimensional cross-linked network that is substantially more stable in strong acid or base than when the peptide film is stabilized by electrostatic interactions alone. Peptide multilayer nanofilms, especially disulfide cross-linked ones, can maintain structural integrity for a long period of time under various conditions. Such knowledge may be pertinent to envisaged applications such as food coatings, medical device coatings, and drug encapsulation.

Supporting Information Available: CD spectra of peptide films treated at various temperatures and in DMF for various times, deconvolution results, UVS spectra of peptide films treated at various pH values for 30 min, and background information on film cross-linking. This material is available free of charge via the Internet at http://pubs.acs.org.

References and Notes

(1) Decher, G.; Hong, J. D.; Schmitt, J. *Thin Solid Films* **1992**, *210/211*, 831.

(2) Balabushevitch, N. G.; Sukhorukov, G. B.; Moroz, N. A.; Volodkin, D. V.; Larionova, N. I.; Donath, E.; Mohwald, H. *Biotechnol. Bioeng.* **2001**, *76*, 207.

(3) Rmaile, H. H.; Schlenoff, J. B. *J. Am. Chem. Soc.* **2003**, *125*, 6602.

(4) Shchukin, D. G.; Shutava, T.; Shchukina, E.; Sukhorukov, G. B.; Lvov, Y. M. *Chem. Mater.* **2004**, *16*, 3446.

(5) Zheng, H. P.; Rubner, M. F.; Hammond, P. T. *Langmuir* **2002**, *18*, 4505.

(6) Müller, M.; Rieser, T.; Dubin, P. L.; Lunkwitz, K. *Macromol. Rapid Commun.* **2001**, *22*, 390.

(7) Berg, M. C.; Yang, S. Y.; Mendelsohn, J. D.; Hammond, P. T.; Rubner, M. F. *Polym. Mater. Sci. Eng.* **2003**, *88*, 46.

(8) Liu, X.; Bruening, M. L. *Chem. Mater.* **2004**, *16*, 351.

(9) Etienne, O.; Picart, C.; Taddei, C.; Haikel, Y.; Dimarcq, J. L.; Schaaf, P.; Voegel, J. C.; Ogier, J. A.; Egles, C. *Antimicrob. Agents Chemother.* **2004**, *48*, 3662.

(10) Caruso, F.; Caruso, R.; Möhwald, H. *Science* **1998**, *282*, 1111.

(11) Rouse, J. H.; Lillehei, P. T. *Nano Lett.* **2003**, *3*, 59.

(12) Watanabe, S.; Regen, S. L. *J. Am. Chem. Soc.* **1994**, *116*, 8855.

(13) Elbert, D. L.; Herbert, C. B.; Hubbell, J. A. *Langmuir* **1999**, *15*, 5355.

(14) Serizawa, T.; Yamaguchi, M.; Akashi, M. *Biomacromolecules* **2002**, *3*, 724.

(15) Kharlampieva, E.; Sukhishvili, S. A. *Langmuir* **2003**, *19*, 1235.

(16) Zhi, Z.; Haynie, D. T. *Macromolecules* **2004**, *37*, 8668.

(17) Richert, L.; Engler, A. J.; Discher, D. E.; Picart, C. *Biomacromolecules* **2004**, *5*, 1908.

(18) Decher, G. *Science* **1997**, *227*, 1232.

(19) Rosenheck, K.; Doty, P. *Proc. Natl. Acad. Sci. U.S.A.* **1961**, *47*, 1775.

(20) Sreerama, N.; Woody, R. W. *Anal. Biochem.* **2000**, *282*, 252 and references therein.

(21) Lvov, Y. In *Protein Architecture: Interfacing Molecular Assemblies and Immobilization Technology*; Marcel Dekker: New York, 2000; pp 125−167 and references therein.

(22) Hartgerink, J.; Beniash, E.; Stupp, S. *Science* **2001**, *294*, 1684.

(23) Li, B.; Haynie, D. T. *Biomacromolecules* **2004**, *5*, 1667.

(24) van Holde, K. E. *Physical Biochemistry*, 2nd ed.; Prentice Hall: Englewood Cliffs, NJ, 1985; pp 77−78.

(25) Creighton, T. E. *Proteins: Structures and Molecular Properties*, 2nd ed.; Freeman: New York, 1993; p 287.

(26) Cooper, A.; Eyles, S. J.; Radford, S.; Dobson, C. M. *J. Mol. Biol.* **1992**, *225*, 939.

(27) Park, M. K.; Xia, C. J.; Advincula, R. C.; Schutz, P.; Caruso, F. *Langmuir* **2001**, *17*, 7670.

(28) Chen, J. Y.; Luo, G. B.; Cao, W. X. *Macromol. Rapid Commun.* **2001**, *22*, 311.

(29) Vuillaume, P. Y.; Jonas, A. M.; Laschewsky, A. *Macromolecules* **2002**, *35*, 5004.